FISEVIER

Contents lists available at ScienceDirect

### **Materials Characterization**

journal homepage: www.elsevier.com/locate/matchar



# Digital identification scheme for steel microstructures in low-carbon steel



Hidenori Terasaki<sup>a</sup>, Yu Miyahara<sup>a</sup>, Kotaro Hayashi<sup>b</sup>, Koji Moriguchi<sup>b</sup>, Shigekazu Morito<sup>c</sup>

- a Faculty of Advanced Science and Technology, Kumamoto University, 2-39-1 Kurokami, Kumamoto 860-8555, Japan
- <sup>b</sup> Technical Research & Development Bureau, Nippon Steel & Sumitomo Metal Corporation, 20-1 Shintomi, Futtsu, Chiba 293-8511, Japan
- <sup>c</sup> Department of Materials Science, Shimane University, 1060 Nishikawatsu, Matsue, Shimane 690-8504, Japan

#### ARTICLE INFO

#### Keywords:

Identification scheme for steel microstructure Kurdjumov–Sachs orientation relationship variants

Phase transformation

#### ABSTRACT

This study proposes a scheme for digital identification of a steel microstructure based on crystallographic features. A 2D space for classifying mixed microstructures of bainite and martensite formed by seven different thermal cycles is defined using two dimensions related to variants in Kurdjumov–Sachs orientation relationships and dislocations. As a dimension relating to variants, the minor variant pair characterized by a rotation axis of  $\langle 011 \rangle$  and a rotation angle of  $52^\circ$  is most useful in classifying the steel microstructure. Furthermore, the kernel average misorientation also served as a suitable dimension for the 2D space. The reasons for using the minor variant pair to classify steel microstructures are discussed from the viewpoint of phase transformation phenomena. The present study demonstrates the possibility for steel microstructures to be digitally identified.

#### 1. Introduction

Various microstructures can be designed using different thermal cycling procedures in low-carbon steel as a result of phase transformations, which enables control of a wide range of mechanical properties such as tensile strength. Recent demand for high-strength steel structures has resulted in a tendency toward using mixed microstructures of bainite (upper and lower bainite) and martensite. Therefore, understanding and classifying the mixed microstructures of bainite and martensite formed by various thermal cycling procedures is essential.

A bainite classification scheme based on carbide precipitate morphology has been suggested [1]. Another classification scheme is based on bainitic ferrite morphology [2]. In low-carbon steel, martensite has a single morphology known as lath martensite and no carbide is observed. These classification schemes were developed from the perspective of morphology. A classification scheme based on carbide morphology is particularly effective. However, the application of electron backscattering diffraction (EBSD) methods to analyze steel microstructures [3-13] enables a statistical microstructural classification scheme based on crystallographic features and suitable for novices. Takayama et al. [13] investigated the frequency of variant pairs in Kurdjumov-Sachs orientation relationships (KSORs) in the transformation temperature range for bainite and martensite in low-carbon steel. By focusing on four variant pairs in one packet, they noted that the variant-pair frequency varied strongly among bainite formed at high temperatures, bainite formed at low temperatures, and martensite.

These four variant pairs are referred to as V1–V2, V1–V3/5, V1–V6, and V1–V4 according to the definition proposed by Morito et al. [14] They clarified that the V1–V4 pair with low-angle boundaries dominates in bainite at high temperatures and that the V1–V2 pair with high-angle boundaries increases and V1–V4 decreases with decreasing transformation temperature. In martensite, the V1–V4 pair again increases, reflecting sub-block formation [14]. Morito et al. [15] demonstrated a simpler method for assessing variant-pair frequencies using block boundary profiles. Their method enables the variant frequency to be quantitatively analyzed over a wide area using EBSD data.

The aforementioned studies provide a basis for the digital classification of steel microstructures, including mixed microstructures, from a crystallographic perspective. The digital classification scheme has opened doors for the automatic recognition of steel microstructure and/or automatic prediction of mechanical properties of steel based on the recognition of mixed-steel microstructure, using artificial intelligence. In order to achieve the scheme, steel microstructure including mixed microstructure should be evaluated in feature space defined by dimensions (feature vector) that characterize the steel microstructures.

In the present study, a 2D space to classify the mixed microstructures comprising bainite and martensite formed during seven thermal cycles using a low-carbon steel were suggested and a method for digital classification in the 2D space is proposed. The results show that the minor variant pair (V1–V6) plays an important role in classifying steel microstructures.

E-mail addresses: terasaki@mech.kumamoto-u.ac.jp (H. Terasaki), 163d8549@st.kumamoto-u.ac.jp (Y. Miyahara), hayashi.fe7.kohtaro@jp.nssmc.com (K. Hayashi), moriguchi.5ym.kohji@jp.nssmc.com (K. Moriguchi), mosh@riko.shimane-u.ac.jp (S. Morito).

<sup>\*</sup> Corresponding author at: 2-39-1 Kurokami, Kumamoto 860-8555, Japan.

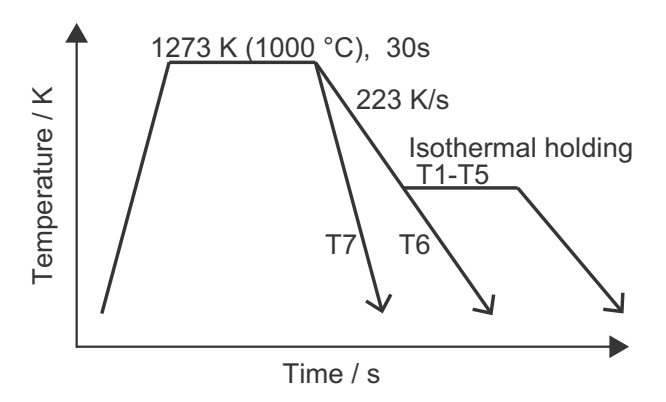


Fig. 1. Diagram of various applied thermal cycles (T1-T7).

#### 2. Experimental Procedures

A low-carbon steel with a composition of Fe-0.1 C-0.01 Si-2.0 Mn-0.008 P-0.001 S (mass pct) was used. Plate specimens 200 mm in length, 20 mm in width and 2.0 mm thickness were cut from the hotrolled flat bar and heat treated using electrical heating apparatus. It was austenitized at 1273 K (1000 °C) for 30 s and then subjected to seven different thermal cycles. Fig. 1 shows the seven thermal cycles, which are referred to as T1-T7. In cycle T7, the steel was cooled to room temperature at the maximum rate using helium gas. In cycle T6, the steel was cooled to room temperature at a rate of 50 K/s. In cycles T1-T5, the steel was cooled at 50 K/s and then maintained at a given temperature shown in Table 1. The holding time for T1-T5 was 1000 s. The samples were subsequently cooled to room temperature, as shown in Fig. 1. These seven thermal cycles produced seven different steel microstructures to be classified. The martensite fraction (other microstructure was bainite) for each cycle was estimated via dilatation method and it was summarized in Table 2. The microstructures are referred to by the abbreviations for the corresponding thermal cycles (T1-T7) in the present study.

After conventional metallographic preparation, polished surface (quarter with reference to the original surface) were etched with 3% nital for subsequent optical microscopy and scanning electron microscopy (SEM). A SEM equipped with a TSL EBSD system was used at an accelerating voltage of 15 kV and a step size of 100 nm. The analyzed area was 12,800 µm, which gave statistical microstructural data corresponding to the applied thermal cycle. No cleanup was performed on the as-acquired dataset. Using EBSD data, the boundaries of six variant pairs in KSORs were visualized. Furthermore, the variant-pair density was quantified by dividing the variant-pair boundary lengths by the observation area with resulting units of  $\mu m^{-1}$ . The variant-pair names (boundary color), misorientation angles between variant pairs, and rotation axes proposed by Morito et al. [15] are summarized in Table 3. The misorientation angle was defined to consider the shift from the ideal KSOR condition, which is often observed in experiments involving low-carbon steel [14,16]. A kernel average misorientation (KAM) was derived using a third-generation condition and a maximum misorientation of 2° because the mode value of the misorientation angle distribution of lath boundaries measured by TEM Kikuchi pattern analysis was approximately 1.5° [17].

 Table 1

 Isothermal holding temperature for applied thermal cycles.

Thermal cycle	Isothermal holding temperature
T1	773 K (500 °C)
T2	723 K (450 °C)
T3	673 K (400 °C)
T4	623 K (350 °C)
T5	573 K (300 °C)

Table 2
Martensite fractions for applied thermal cycles.

Thermal cycle	Martensite fraction/%	
T1	0	
T2	2.1	
T3	63.6	
T4	63.9	
T5	62.2	
T6	70.0	
T7	97.8	

Table 3
KSOR variant-pair names, rotation axes, and misorientation angles proposed by Morito et al. [15].

Variant pair name (in boundary color)	Misorientaion angle between variant pair (Shifted from just KSOR)/degrees	Rotation axis
V1–V2	68	<011>α′
V1-V3/V5	60	<011>α′
V1-V6	52	<011>α′
	7	<011>α′

#### 3. Results and Discussion

Figs. 2 and 3 show optical microscope and SEM images, respectively, for samples T1–T7. In samples T1 and T2, large blocks and chunks of a second phase were observed. By contrast, fine-scale blocks and second-phase particles were detected in samples T3–T7. Such large changes in block and second-phase size are easy to track qualitatively. However, more experience is needed to classify microstructures between samples T1 and T2 and among samples T3–T7 at this observation scale. Our objective was to find a quantitative method for classifying the steel samples' microstructures.

Fig. 4 shows the results of Vickers hardness tests for samples T1–T7. The Vickers hardness is an effective mechanical parameter used to classify steel microstructures. Thus, it can be used to quantitatively classify the microstructures among samples T1, T2, and T3, as shown in Fig. 3; however, its use in classifying microstructures among samples T4–T7 remains difficult.

To quantitatively classify the steel microstructures, we propose a classification space with two dimensions. One of the chosen dimensions is the variant-pair density. Fig. 5 shows an inverse pole figure map for samples T1–T7, and Fig. 6 shows variant-pair boundaries superimposed on the image quality map. The variant-pair boundaries for V1–V2, V1–V3/V5, V1–V6, and V1–V4 are visualized using red, green, blue, and yellow lines, respectively. Fig. 5 shows that the block size decreases with decreasing transformation temperature, as expected. This trend is supported by the variant-pair boundary distribution shown in Fig. 6. As shown in Fig. 6(a), the V1–V4 pair (yellow line) with low misorientation angles was the majority pair in sample T1 and the total amount of variant-pair boundaries was less than in the other samples. With decreasing transformation temperature, the V1–V2 pair (red line) with high misorientation angles and the total amount of variant-pair densities both increase.

To quantitatively analyze the variant-pair density, Fig. 7 shows the variant-pair density distributions measured from Fig. 6 for samples T1–T7. As shown by Takayama et al. [13], the V1–V2 pair and the V1–V4 pair show large changes with decreasing transformation temperature. The V1–V4 pair is abundant in T1, whereas the V1–V2 pair increases and the V1–V4 pair decreases as the transformation temperature decreases, as shown in the case of sample T2. As transformation temperature decreases further, the V1–V2 pair increases further and the V1–V3/V5 pair increases as shown in the case of sample T3. In the case of samples T3–T7, the V1–V4 pair again increases, reflecting increasing

## Download English Version:

# https://daneshyari.com/en/article/5454873

Download Persian Version:

https://daneshyari.com/article/5454873

<u>Daneshyari.com</u>